Fuel 89 (2010) 176–184

Contents lists available at ScienceDirect

Fuel

journal homepage: www.elsevier.com/locate/fuel

Synthetic fuel production from tea waste: Characterisation of bio-oil and bio-char

Başak Burcu Uzun [a,*], Esin Apaydin-Varol [a], Funda Ateş [a], Nurgül Özbay [b], Ayşe Eren Pütün [a]

[a] Anadolu University, Dept. of Chemical Engineering, Iki Eylul Campus, 26480 Eskisehir, Turkey
[b] Bilecik University, Faculty of Engineering, Dept. of Chemical and Process Engineering, Bilecik, Turkey

ARTICLE INFO

Article history:
Received 2 September 2008
Received in revised form 25 August 2009
Accepted 26 August 2009
Available online 9 September 2009

Keywords:
Tea waste
Bio-char
Bio-oil

ABSTRACT

The pyrolysis of tea waste was studied for determining the main characteristics and quantities of liquid and solid products. Particular investigated process variables were temperature (673–973 K), heating rate (5–700 K min^{-1}) and nitrogen gas flow rate (200–800 cm^3 min^{-1}). The maximum oil and char yields are 30.4 (773 K) and 43.3% (673 K), respectively. The liquid and its aliphatic sub-fraction were characterized by elemental analysis, FT-IR, ^1H NMR, and GC/MS. The char was characterized with elemental analysis, SEM, BET, and FT-IR techniques. The aliphatic sub-fraction of the obtained bio-oil contains predominantly *n*-alkanes and alkenes, and branched hydrocarbons. According to the experimental results the liquid products can be used as liquid fuels, whereas the solid product seems to be not suitable for adsorption purposes, due to having low surface areas.

1. Introduction

Increasing petroleum prices and energy demand, serious concerns about security of supply and environmental problems are the major drivers in the search for alternative renewable energy sources. Biomass is a primary candidate because of being the only renewable source of fixed carbon, which is essential in the production of conventional hydrocarbon liquid transportation fuels and many consumer goods [1].

Biomass is a mixture of hemicellulose, cellulose, lignin and minor amounts of other organics which each pyrolyses or degrades at different rates and by various mechanisms and pathways. Lignin decomposes over a wider temperature range compared to cellulose and hemicellulose, which rapidly degrade over narrower temperature ranges, hence the apparent thermal stability of lignin during pyrolysis. The rate and extent of decomposition of each of these components depends on the process parameters such reactor (pyrolysis) temperature, biomass heating rate and pressure [2].

Fast pyrolysis, in which an effort is made to maximize the liquid product yield from solid biomass, is a potential candidate for power production. Fast pyrolysis is a high temperature process in which biomass is rapidly heated in the absence of oxygen. As a result, it decomposes to generate mostly vapors, aerosols and some charcoal. Liquid production requires very low vapor residence time to minimize secondary reactions of typically 1 s, although acceptable yields can be obtained at residence times of up to 5 s if the vapor temperature is kept below 773 K [3]. The bio-oil obtained from pyrolysis can be used as a substitute for fossil fuels for power generation or production of value added chemicals such as resins, liquid smoke, adhesives, anhydro-sugars like levoglucosan, binders for palletizing and briquetting of combustible organic waste materials, preservatives, e.g., wood preservative, so on. Moreover, a suitable blend of a pyrolysis liquid with the diesel oil may be used as diesel engine fuels, bio-oils can be used the oil obtained from sewage sludge pyrolysis can be used directly in diesel fuelled engines, the oil may be stored and transported, and hence need not to be used at the production site [4].

The obtained char finds application as ferroalloy, aluminum, copper, tobacco and cement industries; for the production of chemicals, activated carbon, carbon-nano-tubes, and carbon fibers etc. It is very essential that it is a better fuel than the precursor biomass. It could be used as a solid fuel in boilers where bagasse or other biomass is presently burnt. This can be converted into brickets alone or mixed with biomass and can be used as high efficiency fuel in boilers. It can be used further for the gasification process to obtain hydrogen rich gas by thermal cracking [5]. Pyrolysis gas containing significant amount of carbon dioxide along with methane, might be used as a fuel for industrial combustion purposes. Gases are released from the biomass particles and have generally energy content of 3.5–5.0 MJ m^{-3}. These gases can then be used for firing up furnaces or in diesel generators for producing electricity [6].

Turkey is one of world's important tea producers after China, India, Sri Lanka, Kenya, Indonesia, and Vietnam. Tea plantation covers 70,000 hectares in Turkey. Tea plants (*Camellia sinensis* of the family Theaceae) are commonly grown in the Eastern Black Sea region of Turkey and 150,000 tones black tea is manufactured

* Corresponding author. Tel.: +90 2223350580x6514; fax: +90 2223239501.
E-mail address: bbuzun@anadolu.edu.tr (B.B. Uzun).

0016-2361/$ - see front matter © 2009 Elsevier Ltd. All rights reserved.
doi:10.1016/j.fuel.2009.08.040

per year. The factories around Eastern Black Sea produce about 30,000 tones of waste annually. These wastes are not used for any purpose and stored in depository area [7,8].

Although interests are growing in the use of low cost material and abundantly available lignocellulosic materials to produce liquid and gaseous products and activated carbon, there can be found rarely study about tea factory waste about pyrolysis, gasification or carbonization etc. in literature. Guangwen Xu et al. studied the gasification of tea and coffee grounds and obtain high efficiency in H_2 production with a dual fluidized bed gasifier [9]. Yagmur et al. studied the production of activated carbon from waste tea with chemical activation. Their experimental results show that microwave heating influenced the micro pore development over the activated carbon. Their study shows that tea processing waste, which has a very low economical value, may be used effectively for environmental cleaning purposes [10]. However, there are a few studies about liquid fuel production from tea waste. Demirbaş [11] studied flash pyrolysis of hazelnut shell and tea factory waste to obtain liquid fuels in the presence of sodium carbonate.

In this study, tea waste selected as feedstock for bio-fuel production and the aims of the study are: (i) determine the effect of pyrolysis temperature, sweeping gas flow rates, and heating rate on product yields, (ii) characterize the liquid product obtained under optimum pyrolysis conditions to detect if it can be used instead of conventional fossil fuels or chemical feedstocks, and (iii) characterize the solid products, chars, for their possible use of solid fuels.

Table 1
Proximate and ultimate analyses (wt.%) of tea waste.

Proximate analysis (%)	Tea waste
Ash	3.88
Moisture	7.26
Volatile matters	70.29
Fixed carbon	18.57
Holocellulose	31.05
Lignin	25.68
Extractive	13.97
Oil	2.05
Ultimate analysis (%)	
C	48.6
H	5.43
N	3.8
O	42.17
H/C	1.34
O/C	0.65
Empirical formula	$CH_{1.34}N_{0.03}O_{0.65}$
Calorific value (MJ/kg)	16.19

2. Experimental

2.1. Raw material

The waste sample investigated in this study has been taken from a tea factory around Rize located in Black Sea region in northern part of Turkey. Prior to use, the sample was air-dried and grounded in a high-speed rotary cutting mill. The results for proximate and component analysis that were applied to the grounded, air-dried tea waste samples having average particle size of 0.852 mm were given in Table 1. Ash content of tea waste was found to be as 3.88 wt.%. The feedstock moisture was 7.26 wt.%. The raw material consists of 31.05% holocellulose, 25.68% lignin, and 13.97% extractives. Ultimate analysis was performed on tea waste samples to determine the elemental composition. Using elemental analysis results calorific value of tea waste was calculated to be as 16.19 MJ kg^{-1}.

2.2. Pyrolysis

Pyrolysis was carried out in the apparatus given in Fig. 1. The 316 stainless steel tubular reactor was 90 cm in height and has

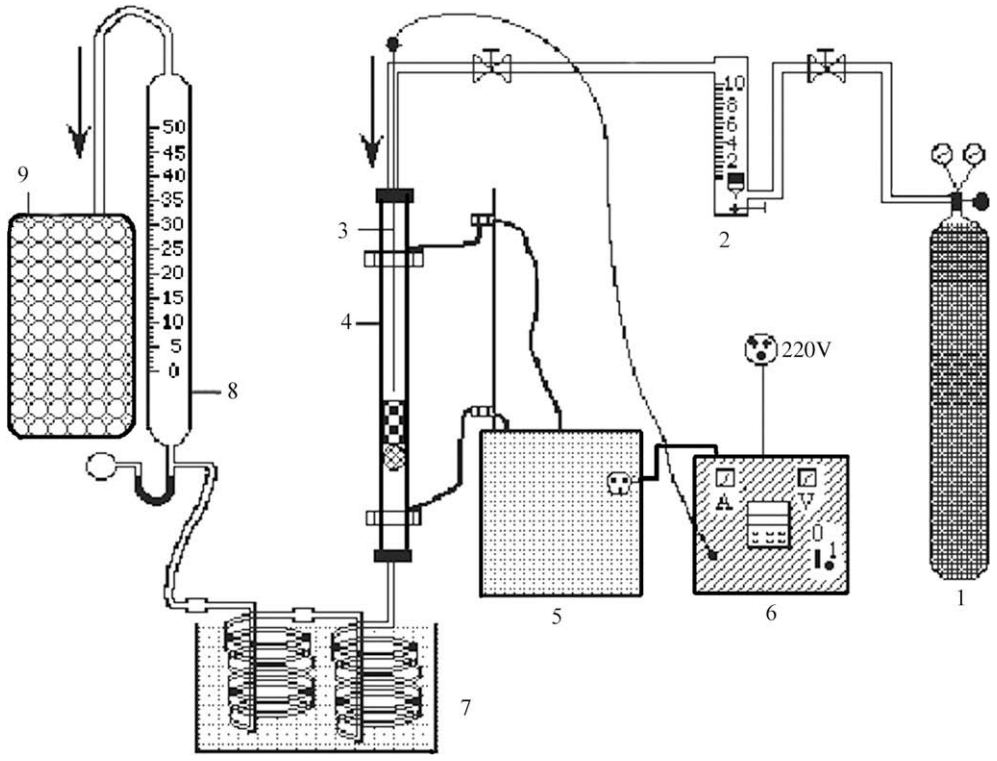

Fig. 1. Schematic diagram of the well-swept fixed-bed tubular reactor. (1) N_2 gas tube; (2) rotameter; (3) thermocouple; (4) reactor; (5) power supply; (6) control unite (7) dry-ice condenser; (8) soap film meter; (9) gas collecting.

2.5 cm internal diameter. A stream of nitrogen was introduced at the top of the reactor and its flow rate was adjusted with a rotameter. Heating rate and pyrolysis temperature were controlled with PID controller.

To determine the effect of the pyrolysis temperature on pyrolysis yields, a 5 g of air-dried sample was placed into the reactor and a sweep gas flow rate of 200 $cm^3\ min^{-1}$ was controlled and measured with a rotameter. The sample was heated with a heating rate of 300 K min^{-1} up to the selected final pyrolysis temperatures of either 673, 773, 823, 973 K and held at that temperature for 10 min or until no further significant release of gas was observed. The second group of experiments was performed to determine the effect of sweeping gas flow rate on pyrolysis oil yield by taking into account the highest oil yields of the first group of experiments. The experiments were carried out to the final temperature of 773 K with a heating rate of 300 K min^{-1} with a sweeping gas flow rate of either 100, 200, 400, 800 $cm^3\ min^{-1}$. The third group of experiment was performed to establish to see the effect of heating rate on the pyrolysis yields. These experiments were conducted with four different heating rates (5, 300, 500, 700 K min^{-1}) with a final temperature of 773 K and sweeping gas flow rate of 200 $cm^3\ min^{-1}$. The volatile products passed through three traps, which were placed in an ice bath. Liquid products were condensed in dry-ice cooled traps and recovered with DCM (dichloro methane) washing. The aqueous layer was separated from organic layer with a separating funnel. The solvent was removed in a rotary evaporator at 313 K and the residual was weighed as the oil. The residual solid in the reactor was weighed as char. The gas yield was calculated by taking the difference.

2.3. Thermal analysis

The thermal behavior of tea waste to 1473 K was studied using Linseis Thermowaage L 81 thermogravimetric analyzer. The sample is suspended by a microbalance located above an electrically heated reactor. Temperature of the sample is measured by a thermocouple that is located near the sample. Al_2O_3 crucibles without lids were used in order to achieve the best possible heat transfer between the thermocouples and crucibles. Gas flow equipment is added to the thermogravimetric analyzer. The gas comes into the upper area of the protection tube via inlet, flows around the sample and reference and leaves via outlet. The gas is heated up when it flows in a pipe through the hot area, flows from up to down over the sample and is sucked of at lower end of the protection tube.

2.4. Characterization

2.4.1. Bio-oil characterization

Bio-oil obtained at the pyrolysis final temperature that gave maximum oil yield, i.e. optimum temperature, was characterized. Elemental analyses (Carlo Erba, EA 1108) were carried out on bio-oil samples. The elemental composition and calorific value of the bio-oil was determined. The chemical class compositions of the oils were determined by liquid column chromatography technique. The oils were first separated into *n*-pentane soluble and insoluble compounds (asphaltenes), of which the *n*-pentane soluble compounds were further separated by adsorption chromatography. Glass column used was packed with silica gel 70–230 mesh, pre-treated at 378 K for 2 h prior to use. The column was eluted successively with 150 mL *n*-pentane, 200 mL toluene and 200 mL methanol to produce aliphatic, aromatic, and polar sub-fractions, respectively. Each fraction was dried and weighed. The FT-IR spectra of the oils and their aliphatic, aromatic and polar sub-fractions were recorded using a Bruker Tensor 27 Model Fourier Transform Infrared Spectrometer. GC–MS analysis of the aliphatic sub-fraction was performed using a Hewlett–Packard 6890 Model gas chromatograph equipped with a 5973 mass selective detector using HP 5 column.^{1}H NMR spectra of the oil were recorded using at 400 MHz, Bruker DPX-400, High performance digital FT-NMR spectrometer for 20 wt.% vol^{-1} solutions in chloroform-d containing TMS (tetramethylsilane) an internal standard.

2.4.2. Char characterization

The elemental analyses of the chars were performed with a Carlo Erba 1108 Elemental Analyzer. The FT-IR spectra of the produced chars was recorded in the transmission mode between 4000 and 400 cm^{-1} using a Bruker Tensor 27 Model Fourier Transform Infrared Spectrometer. Dried KBr was used to prepare pellets from chars.

The surface area of chars was measured in automated volumetric gas adsorption apparatus (Quantochrome Co., Autosorb 1 C) using nitrogen as an adsorbate at 77 K. Before adsorption measurement, the sample was out gassed at 393 K for 3 h. The surface characteristics of the chars were analyzed using Scanning Electronic Microscope Jeol Camscan.

3. Results and discussion

3.1. Thermal analysis

Fig. 2 shows the thermogravimetric (TG) and derivative thermo gravimetric (DTG) curves of tea waste pyrolysed under inert atmosphere for the final temperature of 1473 K heating rate of 10 K min^{-1}. From the DTG curves, the first step mass loss gives its maximum peak at about 373 K. Second weight loss of tea waste starts at about 463 K, having its maximum point at 593 K, finishes at about 623 K. After this temperature, there is essentially no further loss of weight. Biomass is typically composed of cellulose, hemicellulose and lignin. It is known from previous studies that hemicellulose begins to thermally decompose at 423–623 K, and cellulose degradation appears between 548 and 623 K. However lignin degradation takes place at 473–973 K. According to these results, it can be said that since most of the weight loss, related to volatilization of hydrocarbons, happens at temperatures lower than 873 K, choosing pyrolysis temperature as 773 K is appropriate to production of liquid products [12–14].

3.2. Pyrolysis yields

Pyrolysis of tea waste was carried out in three groups of experiments to investigate the effect of pyrolysis conditions on the product yields and to determine the pyrolysis conditions that give the maximum bio-oil yield. To determine the effect of pyrolysis temperature on pyrolysis products yields, the experiments were conducted with a heating rate of 300 K min^{-1}, sweeping gas flow rate of 200 $cm^3\ min^{-1}$and at final temperatures of 673, 773, 823, 973 K. Results of the experiments are given in Fig 3. As can be seen, the char yield decreased from 43.37% to 21.05%, as the final pyrolysis temperature was raised from 673 to 973 K. On the contrary, gas yield increased from 19.99% to 38.26% with the same temperature increase. Its yield was 25.07% at the pyrolysis temperature of 673 K; it appeared to go through a maximum of 29.62% at the final temperature of 773 K. At pyrolysis temperature of higher than 773 K, the oil yield again decreased to a value of 25.84%. It is concluded that the optimum temperature for oil production was 773 K in the present experimental conditions.

The pyrolysis atmosphere can affect both the quantity and quality of all products. The use of inert gases is of major interest in tubular reactors used in this type of processes as predicted in literature. In addition, nitrogen flow influence the residence time of the

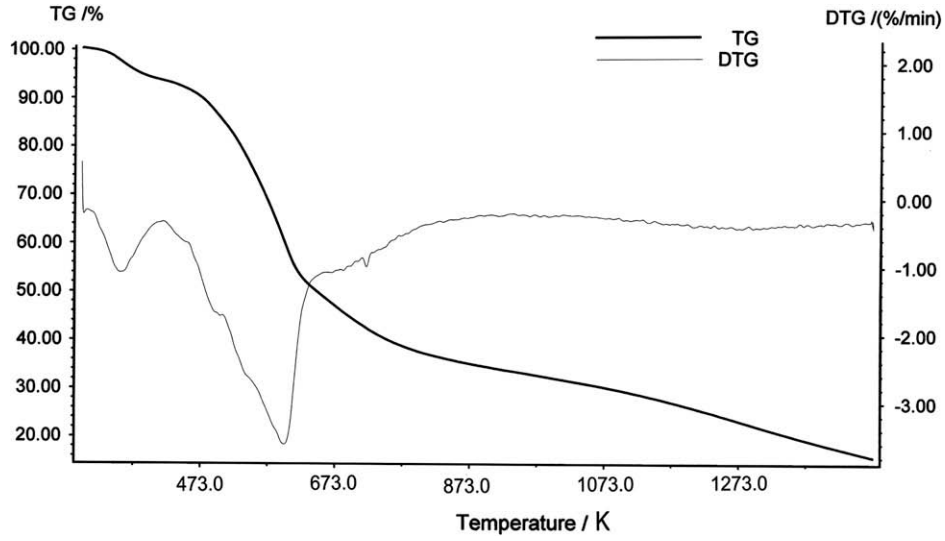

Fig. 2. The thermogravimetric (TG) and derivative thermogravimetric (DTG) curves.

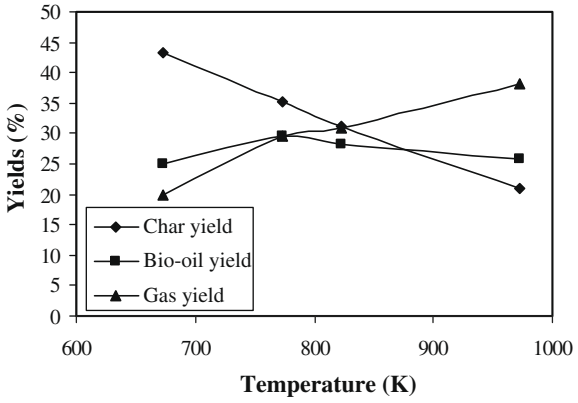

Fig. 3. Yields of pyrolysis products at final temperatures of 673, 773, 823, and 973 K.

vapor phase produced by pyrolysis and prevents the secondary cracking reactions at vapor phase [15]. To determine the effect of the sweeping gas flow rate, a second group experiments were conducted at nitrogen flow rates of 100, 200, 400, 800 $cm^3\ min^{-1}$ to a final pyrolysis temperature of 773 K, with a heating rate of 300 K min^{-1}. The product yields of pyrolysis in relation to flow rate of sweeping gas are given in Fig. 4. It was shown that there was no obvious influence on the char yields as the flow rate of nitrogen increased. The maximum oil yield was 29.62% with a sweeping gas flow rate of 200 $cm^3\ min^{-1}$. In the present study, the maximum oil yield obtained at 200 $cm^3\ min^{-1}$ instead of 800 $cm^3\ min^{-1}$. This can be occurred due to the experimental conditions, especially insufficient quenching. As reported in the literature, sweeping gas at high flow rates causes short residence times of pyrolysis vapors in the reactor. Short residence time of pyrolysis vapors is an important parameter to reach maximum oil yields. But this requires a perfect quenching of thermally cracked pyrolysis vapors. Because of rapid quenching stops the chemical reactions before the valuable initial reaction products can be degraded [16,17].

Heating rate has been studied because previous work has shown that it could have some influence on conversion and product distribution. In addition, heating rate would be an important parameter in possible commercial applications because it would depend on the reactor used [18]. The third group of experiment was performed to establish the effect of heating rate on the pyrolysis yields. These experiments were conducted with four different heating rates of 5, 300, 500, 700 K min^{-1} with a final temperature of 773 K and a sweeping gas flow rate of 200 $cm^3\ min^{-1}$. Experimental results are given in Fig. 5. As the residence times are getting longer, secondary reactions such as dehydration, decarboxylation and condensation will occur. It is evident that fast pyrolysis units produce higher liquid products than slow pyrolysis units. As can be seen, higher heating rates caused a sharp increase in the yield of liquid products because of reduced heat and mass transfer

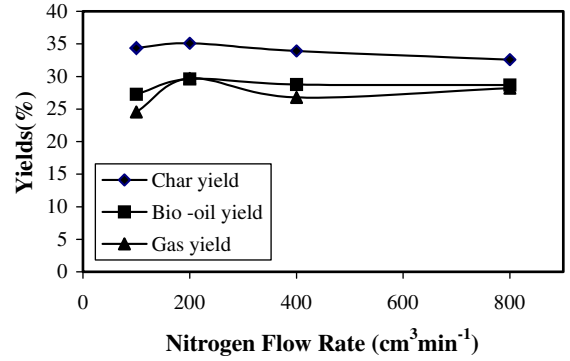

Fig. 4. Yields of pyrolysis products at sweeping gas rates of 100, 200, 400, and 800 $cm^3\ min^{-1}$.

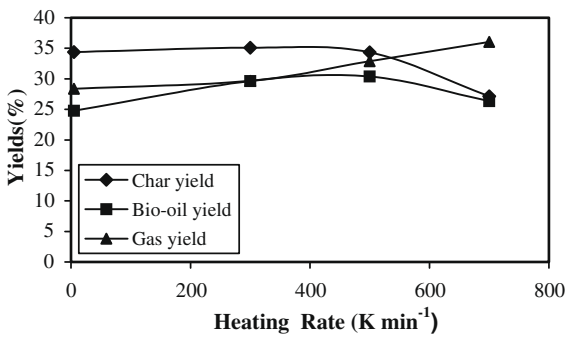

Fig. 5. Yields of pyrolysis products at heating rates of 5, 300, 500, and 700 K min^{-1}.

Table 2
Elemental analysis results for the bio-oil and its sub-fractions (wt.%).

Component	Bio-oil	Aliphatics	Aromatics	Polars
C	69.26	84.53	77.39	71.49
H	8.97	15.47	9.42	9.27
N	6.19	–	0.93	3.80
O*	15.58	–	12.26	15.45
H/C	1.54	2.18	1.45	1.54

limitations, resulting in maximum oil yields. Increasing heating rate from 5 to 500 K min^{-1} resulted in an increase of bio-oil yield up to 22.73%. The char yield decreased from 34.3% to 27.1%, when the heating rate was raised from 5 to 700 K min^{-1}.

3.3. Bio-oil characterization

The typical bio-oil is brown colour and contains 10–25 wt. of water. In our study, the liquid product obtained at 773 K is red-brown-colour and consists of ca. 10 wt.% of water [19]. Calorific values of bio-oils obtained from fast pyrolysis are found to be as 29.59 MJ kg^{-1}. Because of having high calorific values, pyrolytic oils can be used as fuels for combustion systems in industry [20].

Pyrolytic oils are complex mixtures consisting of organic compounds from wide variety of chemical groups. To characterize the pyrolytic oil, the oils were separated into four fractions; asphaltenes, aliphatics, aromatics and polars. The results of the adsorption chromatography of the oil showed that the pyrolysis oil consists of 54% *n*-pentane soluble and the rest is asphaltenes. The aliphatic, aromatic, and polar fractions of the *n*-pentane soluble were 20, 25, and 55%, respectively.

The elemental compositions of bio-oils and sub-fraction are given in Table 2. Bio-oil contains less amounts of oxygen content than that of the original feedstock. The significant decrease in oxygen content of the oil compared to the original feedstock is important, because the high oxygen content is not attractive for the production of transport fuels [21]. As seen, aliphatic sub-fraction has no oxygen with high hydrogen content. Moreover, H/C ratios of bio-oil and *n*-pentane sub-fraction are 1.54 and 2.18, which is very close to that of gasoline.

Biomass pyrolysis oils contain a very wide range of complex organic chemicals [22–23]. FT-IR spectra of the bio-oil and its sub-fractions are shown in Fig. 6. The O–H stretching vibrations between 3200 and 3400 cm^{-1} indicate the presence of phenols and alcohols. The figure shows that no peak exists between these wave numbers for the aliphatic sub-fraction of bio-oil, and this indicates that aliphatic sub-fraction does not contain oxygenated compounds like bio-oil, and this result obtained in the present study was also in consistent with elemental and GC/MS analysis.

The C–H stretching vibrations between 2850 and 2925 $cm^{-1}$and C–H deformation vibrations between 1350 and 1475 cm^{-1} indicate the presence of alkanes. Moreover, the location of bending vibration of C–H groups at 1378 cm^{-1} provides another evidence of the fact that this band is very important for the detection of methyl groups in a given compound. Carbonyl stretching absorptions cause the band at about 1745 cm^{-1} in the spectrum. In addition,

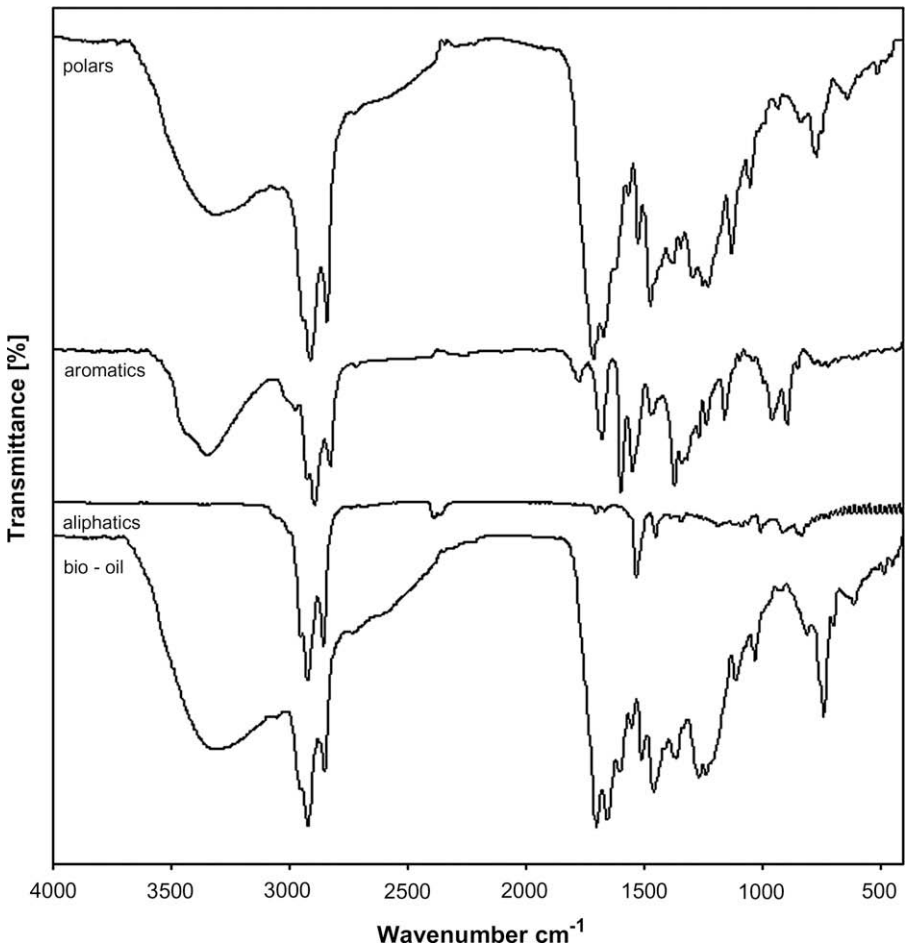

Fig. 6. FT-IR spectra of the bio-oil and its column chromatographic sub-fractions.

Table 3
Hydrogen type distribution of oil from ^{1}H NMR spectra.

Hydrogen type	Chemical shift (ppm)	Oil*
CH_3 γ or further from aromatic ring and paraffinic CH_3	1.0–0.5	8.83
CH_3; CH_2 and CH β to aromatic ring	1.5–1.0	23.82
CH_2 and CH attached to naphthenes	2.0–1.5	6.22
CH_3; CH_2 and CH α to aromatic or aceytlenic	3.0–2.0	25.44
Total aliphatics	3.0–0.5	64.31
Hydroxyl, ring-joining metylene, methine or methoxy	4.0–3.0	7.73
Phenols, non-conjugated olefins	6.0–4.0	10.19
Aromatics, conjugated olefins	9.0–6.0	17.78

* Oil obtained at optimum conditions.

Table 4
Identification and yield (area%) of *n*-pentane sub-fraction.

Product	Area (%)
Undecane	1.36
1-Decene	1.34
Dodecane	2.12
1-Tridecene	1.66
Tridecane	2.82
1-Tetradecene	2.43
Tetradecane	3.38
1-Pentadecene	1.95
Pentadecane	4.78
3-Hexadecene	1.46
Hexadecane	1.98
1-Heptadecene	1.24
Heptadecane	1.86
1-Heptene,2isohexyl-6methyl	1.84
1-Octadecene	1.42
Octadecane	1.60
2-Nonadecene	1.03
Nonadecane	1.70
5-Eicosene	1.41
Eicosane	2.59
Heneicosane	2.71
5-Eicosene	1.39
Docosane	3.67
1-Docosene	1.11
Tetracosane	5.63
Pentacosane	7.35
Hexacosane	8.11
Heptacosane	7.62
Octacosane	6.94
Nonacosane	6.65
Total	
n-Alkanes	72.87
n-Alkenes	16.44
Branched	1.84

the presence of these peaks together with the presence of C=C stretching vibrations between 1680 cm^{-1} and 1700 cm^{-1} is compatible with the presence of ketone, quinone, aldehyde groups etc.

Aromatic ring C–H stretching vibration 3000 cm^{-1} and stretching vibration of aliphatic bonding to the aromatic ring at 2923 cm^{-1} are an important evidence of the aromacity of toluene sub-fraction. The region between 700 and 900 cm^{-1} contains various bands related to the aromatic, out of plane C–H bending. The high intensity of above-mentioned bands indicates that the aromatic hydrogen is located in aromatic rings with high degree of substitution. The band in the FT-IR spectrum of toluene sub-fraction indicates higher content of CH_3 groups in the form of aliphatic chains [24].

^{1}H NMR spectroscopy was applied to the bio-oil obtained under optimum conditions. The hydrogen distribution of ^{1}H NMR [25] is given in Table 3. Generally, based on the chemical shifts of specific proton types, ^{1}H NMR spectra can be divided into three main regions; aromatic, olefinic, and aliphatic whose resonances occur in the chemical shift regions of 9.0–6.0, 6.0–4.0 and 3.0–0.5 ppm, respectively. The results showed that larger proportions of aliphatic structural units existed in the bio-oil from fast pyrolysis of tea waste.

Fig. 7 shows the GC/MS spectrum of the aliphatic sub-fraction of pentane soluble bio-oil. The aliphatic fractions consist of *n*-alkanes, alkenes and branched hydrocarbons. The majority of the linear chain hydrocarbons were distributed in the range of C_{11}–C_{29}, but the intensive peak can be considered as C_{11}–C_{18}. In the chromatograms mostly doublet peaks were observed. The first ones belong to *n*-alkenes and the second ones to *n*-alkane [26].

In order to determine the distribution of these hydrocarbons in aliphatic, a semi-quantitative study was made by means of the percentage of area of the chromatographic peaks (Table 4). While considering the results of GC/MS detailed analysis, the total amounts of *n*-alkanes, *n*-alkenes and branched hydrocarbons were 72.87%, 16.44%, and 1.84%, respectively.

3.4. Char characterization

Fig. 8 shows the relationship between the hydrogen/carbon (H/C) and oxygen/carbon (O/C) ratios of the chars. As can be seen, the H/C ratio decreased continuously with increasing temperature i.e. the H/C ratio of char obtained at 673 and 973 K was 0.78 and 0.28, respectively. In addition, the thermal application caused decrease of this ratio i.e. 1.34 for tea waste, 0.28 for char at 973 K.

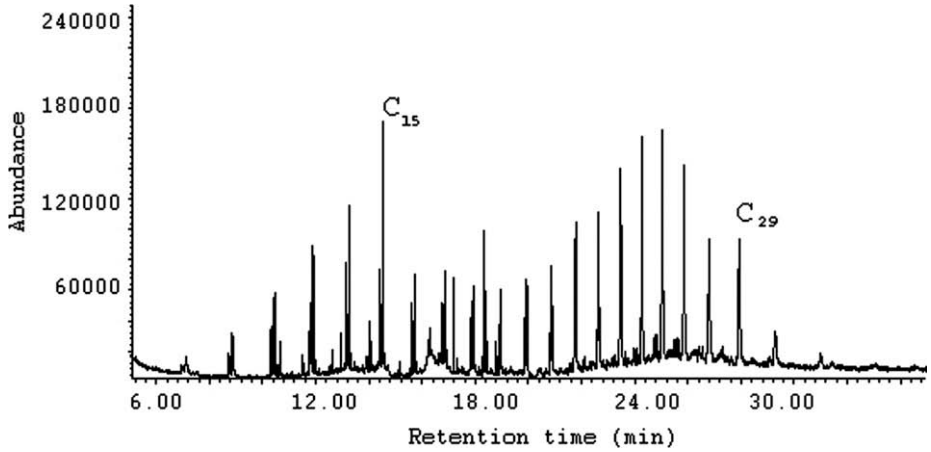

Fig. 7. GC/MS analysis of aliphatic sub-fraction of the bio-oil.

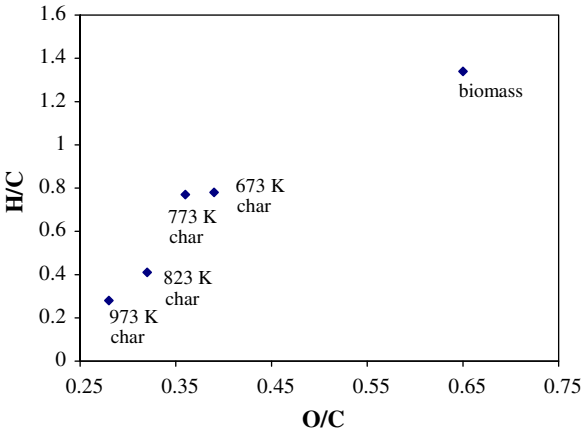

Fig. 8. Van Krevelen diagram for tea waste and its chars obtained at different temperatures.

As the temperature increased, O/C ratio decreased and that the char became increasingly more carbonaceous in nature at high temperatures [27–29].

The infrared spectra of char samples are illustrated in Fig. 9. To improve the spectral quality, bands due to the atmospheric contributions of CO_2 have been subtracted from the spectra. Various bands in the spectra were identified corresponding to stretches hydrogen-bonded OH (3446–3527 cm^{-1}), aromatic CH (3023–3054 cm^{-1}), aliphatic CH_3 (2923–2961 cm^{-1}), aliphatic CH_2 (2870–2988 cm^{-1}), aromatic CH_3, i.e., CH_3 on an aromatic ring (2829–2888 cm^{-1}), C=C (1581–1669 cm^{-1}), and an aromatic CH wag, i.e., an aromatic ring (various bands between 700 and 900 cm^{-1}). The stretches because of the OH and C=O groups in chars showed continuous decrease intensity with temperature, indicating loss of these functionalities at high temperatures. Because OH stretches is affected by inter and intra molecular, hydrogen bonding also changed with pyrolysis temperature [30].The asymmetric and symmetric vibration modes of methyl and methylene groups appeared 2923 cm^{-1} and 2800 cm^{-1} in chars and intensity decreased as temperature increased from 673 K to 973 K and this band was completely disappeared above 773 K. It is clear that high temperatures increase aromaticity while decreasing aliphaticity (Fig. 9).

There are many spectral bands in the region between 1600 and 900 cm^{-1}. The shoulder at ~1581 cm^{-1} is attributable to in-plane skeletal vibrations in aromatic rings. The variations in aromatic

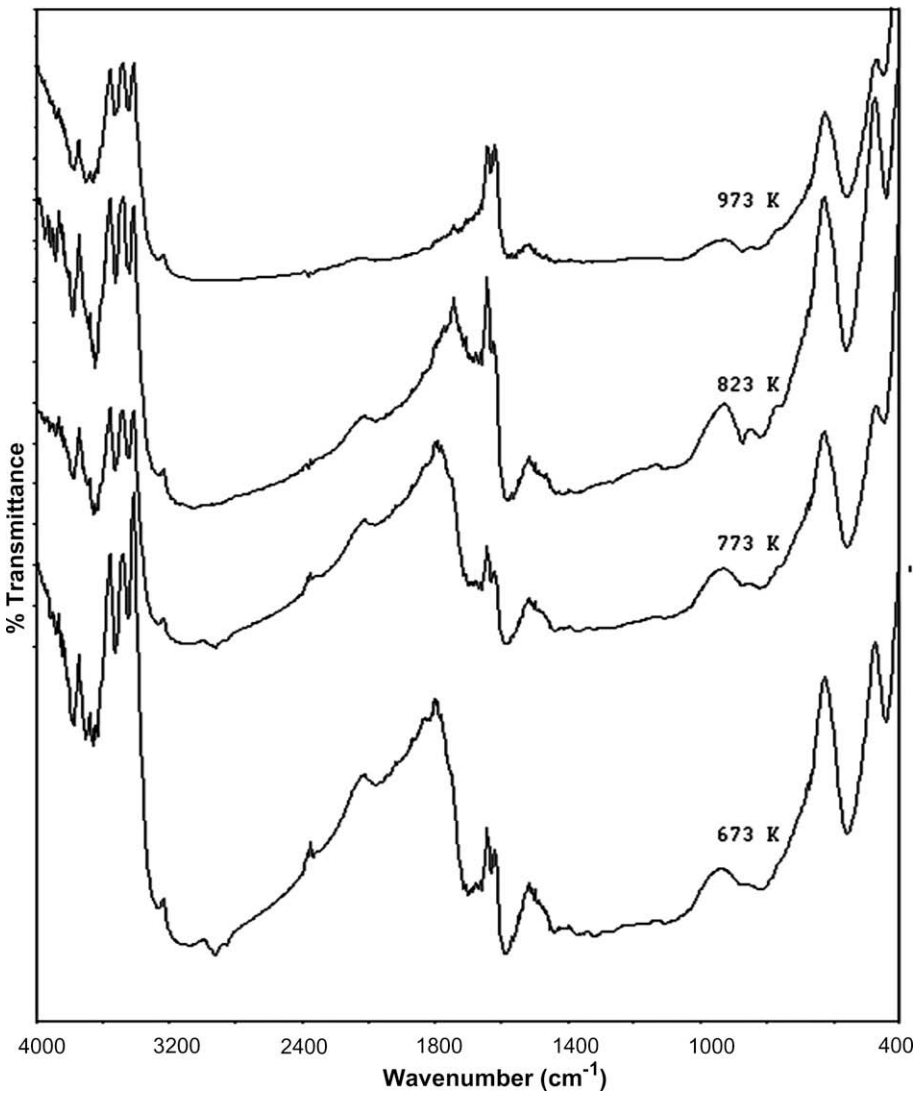

Fig. 9. FT-IR spectra of chars obtained at different temperatures.

CH wags in the 900–700 region were used to study the changes in aromatic structures. The spectrum of the 973 K char showed the disappearance of the most bands and suggested that the char was mainly aromatic polymer carbon atoms [30].

The surface area of char is important because, like other physicochemical characteristics, it may strongly affect the reactivity and combustion behavior of the char. The chars produced at 673 K and 973 K had relatively low surface areas of $\sim$2 $m^2\ g^{-1}$and 7.5 $m^2\ g^{-1}$ (N_2 adsorption at 77 K), respectively. Due to having low surface areas, it could be thought that the chars have low adsorption capacity. Yagmur et al. studied production of activated carbon from tea waste by chemical activation with microwave energy. The surface areas of the raw material and char (from pyrolysis of tea waste at 623 K) were found as 1.18 $m^2\ g^{-1}$ and 1.287 $m^2\ g^{-1}$, respectively. They obtained the maximum surface area as 1157 $m^2\ g^{-1}$ for the sample activated with phosphoric acid and carbonized at 623 K [10].

SEM images confirmed the amorphous and heterogeneous structure of tea waste chars. A comparison of SEM analysis of the chars allows interesting conclusions to be drawn about morphological changes after the devolatilization step. The SEM images of the chars at low and high temperature are given in Fig. 10. It is obvious from a phenomenological point of view, a gradual release of different volatile compounds occurs as the temperature increases during a high heating rate devolatilization. At 673 K, both open and closed vesicles were present. The presence of vesicles indicates that volatile components were formed and released and that the vesicles occurred through plastic deformation, a melt phase of cellular components. The char particles obtained at pyrolysis temperature of 973 K form equant-shape particles may be the result of secondary product formation from the precipitation of volatile gases.

Significantly different is the morphology of the high temperature char particles. In this case the fast volatile release during pyrolysis produces substantial internal overpressure and the coalescence of the smaller pores. This leads to large internal cavities and a more open structure. SEM macroporosity therefore increased with an increasing temperature [31,32].

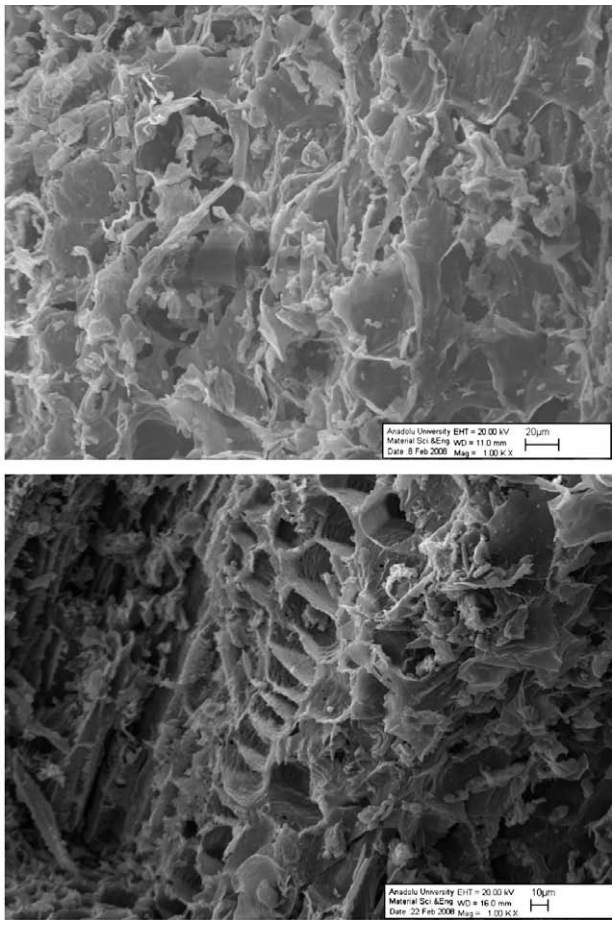

Fig. 10. Scanning electron micrographs (magnification = 1000×) of tea waste char obtained at different pyrolysis temperatures (a) 673 K, (b) 973 K.

4. Conclusion

In this study pyrolysis experiments of tea waste were carried out in a well-swept fixed-bed reactor in order to investigate the effects of pyrolysis temperature, heating rate and sweep gas flow rate on product yields and chemical compositions of the produced liquids. The experimental data obtained showed that the highest yield of pyrolytic oil was obtained as 30% with heating rate of 500 K min^{-1}, at the pyrolysis temperature of 773 K under the nitrogen flow rate of 200 $cm^3\ min^{-1}$. Comparison of H/C ratios with conventional fuels shows that the H/C ratios of the bio-oil obtained in this work is between those of light and heavy petroleum products. The results of the spectroscopic methods are in consistence with chromatography, confirming that the hydrocarbons of the aliphatic fraction of the bio-oil are mixtures of alkanes and alkenes. The yields of the pyrolysis experiments and the result of the spectroscopic and chromatographic methods indicate that the pyrolysis oil can be considered as a potential fuel.

The characteristic of char is dependent on the pyrolysis conditions. Both the hydrogen and oxygen contents of char decrease as the temperature is increased. The FT-IR results showed that the hydroxyl and carbonyl functionalities were lost as the temperature increased. According to BET results, obtained chars at 673 K and 973 K had relatively low surface areas.

References

[1] Gerhauser AH, Bridgwater AV. Production of renewable phenolic resins by thermochemical conversion of biomass. Renew Sust Energ Rev 2008;12:2092–116.
[2] Bridgwater AV. Principles and practice of biomass fast pyrolysis processes for liquids. J Anal Appl Pyrol 1999;51:3–22.
[3] Bridgwater AV, Meier D, Radlein D. An overview of fast pyrolysis of biomass. Org Geochem 1999;30:1479–93.
[4] Goyal HB, Diptendu S, Saxena RC. Bio-fuels from thermochemical conversion of renewable resources. Renew Sust Energ Rev 2008;12:504–17.
[5] Katyal S, Thambimuthu K, Valix M. Carbonisation of bagasse in a fixed bed reactor: influence of process variables on char yield and characteristics. Renew Energ 2003;28:713–25.
[6] Lim MT, Alimuddin Z. Bubbling fluidized bed biomass gasification performance process findings and energy analysis. Renew Energ 2008;33:2339–43.
[7] Malkoc E, Nuhoglu Y. Potential of tea factory waste for chromium(VI) removal from aqueous solutions: thermodynamic and kinetic studies. Sep Purif Technol 2007;54:291–8.
[8] Malkoc E, Nuhoglu Y. Fixed bed studies for the sorption of chromium(VI) onto tea factory waste. Chem Eng Sci 2006;61:4363–72.
[9] Xu G, Murakami T, Suda T, Matsuzawa Y, Tania H. Two-stage dual fluidized bed gasification: its conception and application to biomass. Fuel Process Technol 2009;90:137–44.
[10] Yagmur E, Ozmak M, Aktaş Z. A novel method for production of activated carbon from waste tea by chemical activation with microwave energy. Fuel 2008;87:3278–85.
[11] Demirbaş A. Partly chemical analysis of liquid fraction of flash pyrolysis products from biomass in the presence of sodium carbonate. Energ Convers Manage 2002;43:1801–9.
[12] Ozbay N, Putun AE, Uzun BB, Putun E. Biocrude from biomass: pyrolysis of cottonseed cake. Renew Energ 2001;24:615–25.
[13] Ozbay N, Putun AE, Putun E. Bio-oil production from rapid pyrolysis of cottonseed cake: product yields and compositions. Int J Energy Res 2006;30:501–10.
[14] Putun AE, Ozbay N, Onal EP, Putun E. Fixed-bed pyrolysis of cotton stalk for liquid and solid products. Fuel Process Technol 2005;86:1207–19.
[15] Uzun BB, Putun AE, Putun E. Composition of products obtained via fast pyrolysis of olive-oil residue: effect of pyrolysis temperature. J Anal Appl Pyrol 2007;79:147–53.

[16] Putun AE, Ozbay N, Apaydin-Varol E, Uzun BB, Ates F. Rapid and slow pyrolysis of pistachio shell: effect of pyrolysis conditions on the product yields and characterization of the liquid product. Int J Energy Res 2007;31:506–14.
[17] Maggi R, Delmon B. Comparison between slow and flash-pyrolysis oils from biomass. Fuel 1994;73:671–7.
[18] Uzun BB, Pütün AE, Pütün E. Fast pyrolysis of soybean cake: product yields and compositions. Bioresource Technol 2006;97:569–76.
[19] Mastral AM, Murillo R, Callein MS, Garcıa T, Snape CE. Influence of process variables on oils from tire pyrolysis and hydropyrolysis in a swept fixed bed reactor. Energ Fuel 2000;14:739–44.
[20] Tsai WT, Lee MK, Chang YM. Fast pyrolysis of rice straw, sugarcane bagasse and coconut shell in an induction-heating reactor. J Anal Appl Pyrol 2006;76:230–7.
[21] Ucar S, Karagoz S, Ozkan AR, Yanik J. Evaluation of two different scrap tires as hydrocarbon source by pyrolysis. Fuel 2005;84:1884–92.
[22] Onay O. Fast and catalytic pyrolysis of *Pistacia khinjuk* seed in a well-swept fixed bed reactor. Fuel 2007;86:1452–60.
[23] Vitolo S, Seggiani M, Frediani P, Ambrosini G, Politi L. Catalytic upgrading of pyrolytic oils to fuel over different zeolites. Fuel 1999;78:1147–59.
[24] Putun AE, Onal E, Uzun BB, Ozbay N. Comparison between the "slow" and "fast" pyrolysis of tobacco residue. Ind Crop Prod 2007;26:307–14.
[25] Ozbay N, Uzun BB, Apaydın Varol E, Putun AE. Comparative analysis of pyrolysis oils and its subfractions under different atmospheric conditions. Fuel Process Technol 2006;87:1013–9.
[26] Pindoria RV, Lim JY, Hawkes JE, Lazaro MJ, Herod AA, Kandioti R. Structural characterization of biomass pyrolysis tars/oils from eucalyptus wood waste: effect of H_2 pressure and sample configuration. Fuel 1997;76:1013–23.
[27] Sharma RK, Wooten JB, Baliga VL, Lin X, Chan WG, Hajaligol MR. Characterization of chars from pyrolysis of lignin. Fuel 2004;83:1469–82.
[28] Sharma RK, Hajaligol MR, Mortoglio-Smith PA, Wooten JB, Baliga VI. Characterization of char from pyrolysis of chlorogenic acid. Energ Fuel 2000;14:1083–93.
[29] Sharma RK, Wooten JB, Baliga VI, Mortoglio-Smith PA, Hajaligol MR. Characterization of char from the pyrolysis of tobacco. J Agric Food Chem 2002;50:771–83.
[30] Gomez-Serrano V, Alvarez PM, Jaramillo J, Beltran FJ. Formation of oxygen complexes by ozonation of carbonaceous materials prepared from cherry stones, I. Thermal Effects Carbon 2002;40:513–22.
[31] Guerrero M, Ruiz MP, Alzueta MU, Bilbao R, Millera A. Pyrolysis of eucalyptus at different heating rates: studies of char characterization and oxidative reactivity. J Anal Appl Pyrolysis 2005;74:307–14.
[32] Apaydin-Varol E, Putun E, Putun AE. Slow pyrolysis of pistachio shell. Fuel 2007;86:1892–9.